Flexible Piles within MSE Retaining Wall System

Salah Mahdi Hamza[1], Shaymaa T. Kadhim[1], and Saad F. A. Al-Wakel[1]
[1]*Civil Engineering Department, University of Technology-Iraq, Baghdad, Iraq*
E-mail: salahmahdi020@gmail.com

ABSTRACT: In bridges, pile foundations carry the lateral loads created by the movement of the abutment deck. Due to the limited space, retaining walls constructed of mechanically stabilized earth (MSE) may be constructed on the abutment face. In contrast to conventional design methodologies for MSE retaining walls and piles, the effect of pile-wall interaction must be thoroughly investigated. The effects of several variables on the behavior of a flexible pile subjected to lateral loading and located behind an MSE retaining wall system in loose and dense sand soils are discussed in this study. These variables include the offset of the piles, the slenderness ratio, the soil density, the length of reinforcement, and the type of connection between the reinforcing units and the wall facing. The results indicated that when flexible piles are installed closer to the MSE retaining wall, their lateral capacity is significantly reduced. In comparison to the frictional connection model, the mechanical connection between BRC wire mesh and wall facing exhibited better performance of flexible piles in terms of lateral capacity.

KEYWORDS: Retaining wall, Pile, Lateral resistance.

1. INTRODUCTION

Over the last four decades, MSE retaining walls have been extensively used in geotechnical applications such as bridge abutments and embankments (FHWA, 2007; Berg and Vulova, 2007). Because bridge abutments are supported by pile foundations, piles must be constructed in the reinforced area behind the MSE retaining wall that supports the bridge foundation. In this case, the piles are subjected to lateral loading as a result of the movement of the bridge deck. Due to the limited space within the construction area, piles have been placed within the MSE retaining wall system as they support wind loads like sound walls, traffic signs, and other types of superstructures. These conditions require a different design methodology than MSE walls and pile foundations. The standard practice is to design the pile independently, ignoring the effect of the MSE wall by assuming the pile is fixed into a rock socket or by positioning the pile far enough away from the wall. This results in an increase in the cost of bridge construction (Rollins et al., 2012).

Numerous research studies utilizing full-scale model tests have been conducted (Pierson et al., 2009; Huang et al., 2011; Rollins et al., 2011; Rollins et al., 2012; Price, 2012; Nelson, 2013; Han, 2014; Rollins and Nelson, 2015). Pierson et al. (2009) conducted full-scale lateral loading tests at four locations on 0.9 m diameter piles embedded behind a 6 m high masonry retaining wall and reinforced with geogrids. Nelson (2013) conducted a full-scale study at three locations to determine the lateral load capacity of 0.32 m diameter steel-strip reinforced piles within an MSE wall system. The offsets from the wall facing were investigated at 6.3, 2.7, and 1.3 pile diameter. Rollins et al. (2012) reported that double wrapping the pile with a 0.25 mm thick polyethylene sheet resulted in a significant reduction in the pile's lateral capacity within the MSE retaining wall system used to mitigate drag forces.

Mohammed (2016) examined the performance of a rigid pile with a diameter of 63.5 mm embedded in dense sand behind a geogrid-reinforced MSE retaining wall. It was concluded that the effect of the connection type used to connect the wall facing and geogrid on the rigid pile's lateral capacity is highly dependent on the geogrid layer length. Jawad et al. (2020) simulated the performance of a single pile behind an MSE retaining wall system using small-scale models. The test results indicated that when the pile offset was twice the diameter of the pile, the lateral capacity of the pile decreased by 21%, compared to when the pile offset was four times the diameter of the pile.

Numerous researchers also investigated the pile-MSE wall interaction numerically (Khodair and Hassiotis, 2005; Huang et al., 2013; Wilson et al., 2016). Wilson et al. (2016) conducted a finite element analysis of piles embedded behind an MSE wall that were subjected to longitudinal and transverse loading.

The majority of previous research has focused on the interaction of pile-wall systems in the presence of rigid pile behavior. In this paper, the interaction between the pile and the MSE retaining wall is investigated when the pile is flexible at various slenderness ratios (L/D) and embedded in sand with two different densities (i.e., Dr = 30% and 80%). Several factors affecting the performance of pile foundations under the influence of lateral loads within the MSE retaining wall system were investigated. For example, the pile offset from the retaining wall facing, the pile slenderness ratio, the sand relative density, the reinforcement length, and the type of connection between the BRC layers and the retaining wall facing.

2. MATERIALS AND TEST PROGRAM

2.1 Materials

The results of physical tests conducted on soil are summarized in Table 1, including sieve analysis, minimum and maximum densities, and a direct shear test to determine the angle of internal friction of soil at various sand soil densities (i.e., loose and dense sand). The mean particle size (D_{50}) of the soil was 0.34 mm. The soil was classified as poorly graded sand according to the USCS.

Table 1 Physical testing results of sand used in this study

Physical Properties	Value		Specification
	Loose	Dense	
Relative density (D_r)%	30	80	
dry unit weight, (kN/m^3)	16.43	17.6	
Angle of internal friction(ϕ), deg.	28	36	ASTM D3080-03
D_{10}, (mm)	0.15		ASTM D422 and ASTM D2487
D_{30}, (mm)	0.23		
D_{50}, (mm)	0.34		
D_{60}, (mm)	0.40		
Coefficient of uniformity (Cu)	2.67		
Coefficient of curvature (Cc)	0.88		
Specific gravity (Gs)	2.65		ASTM D854
Maximum dry unit weight, (kN/m^3)	18.05		ASTM D4253
Minimum dry unit weight, (kN/m^3)	15.82		ASTM D4254

As illustrated in Figure 1, this work utilized steel pipe piles with an outer diameter of 20.5 mm, a wall thickness of 0.3 mm, and an elastic modulus of 2.16×10^4 MPa. To accomplish the study's objectives, various pile lengths (i.e., 286, 335.5, and 385 mm) were

prepared. According to Sharma (2011), the pile's slenderness ratio (L/D) varies between (19.3, 21.7, and 24.1), as illustrated in Table 2. The eccentricity of the load (e) was set at 110 mm. Several concrete panels were cut and prepared from larger concrete blocks to represent the face of the MSE retaining wall. Each panel had dimensions of 45, 380, and 50 mm in height, length, and width, respectively. To ensure the wall's internal stability, punched-down BRC with apertures was used. As illustrated in Figure 2, this study used two types of connections between BRC and the retaining wall face: mechanical and frictional connections. To provide a suitable interconnection between the BRC unit and the wall facing, a mechanical connector was used, represented by an aluminium bolt passed through holes and was fastened to the BRC.

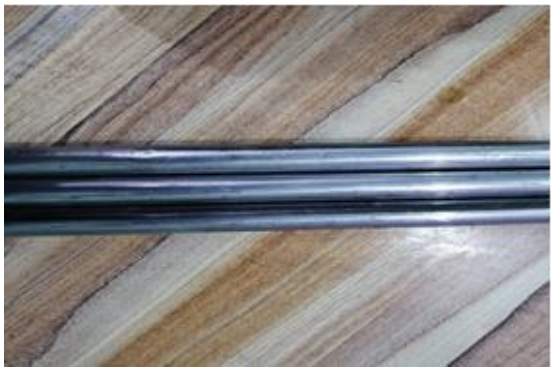

Figure 1 Pipe piles

Table 2 Length to diameter ratios of piles used in this study

L/D	Embedded length of pile, L (mm)	e + L (mm)
19.3	286	396
21.7	335.5	445.5
24.1	385	495

(a)

(b)

Figure 2 Connection types used in this study: (a) Mechanical and (b) Frictional connection

2.2 Instrumentations and Test Setup

The applied lateral load was measured in this study using a digital weighing indicator (SEWHA) with SI (4010r). The digital weighing indicator has an input sensitivity of 0.2 μV/digit, an excitation voltage of DC 10V (± 5V), and a maximum input voltage signal of 32 mV. For tension and compression, an S-beam (SS300) load cell with a maximum capacity of 1000 kg was used. The output rate of the load cell is 2.0±0.005 mV/V with a cumulative error of 0.03%, and the excitation voltage is 10-15V (10 recommended). Additionally, three pressure cells were connected to the interior of the blocks forming the retaining wall in order to detect the amount of lateral pressure behind the retaining wall. At the center of the retaining wall facing, the pressure cells were coordinated. As illustrated in Figure 3, the vertical spacing between the pressure cells was 25%, 50%, and 75% of the retaining wall height measured from the base of the test container. For static loading, the lateral deflection at the pile head was measured using a dial gauge.

The experiments were performed by means of a rectangular-shaped test container with a wooden base. The container's inside dimensions were 830 mm in height, 1400 mm in length, and 400 mm in breadth. The container's front side is made of 10 mm thick tempered glass, while the remaining three sides are made of wooden plates. The upper part of the container can be removed during the test.

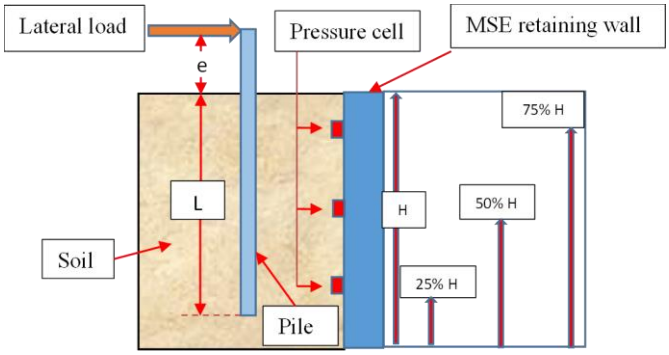

Figure 3 Distribution of pressure cells along the face of retaining wall

The lateral load was applied in accordance with the ASTM (D3966-07) specification for testing deep foundations under lateral load. The system used to apply the lateral loads to the experimental model is depicted in Figure 4. This system uses an iron screw shaft to apply lateral force to the pile cap. The screw shaft was connected to a load cell device that used to determine the applied load. The system consists of gearbox used to move and push the screw shaft forward, along with another gearbox that is used to determine the required velocity. The screw shaft was designed to move very slow to moderate rate of movement. It was programmed in such a way that the rate of movement can be adjusted using an electrical system (AC Drive) to achieve the desired rate of movement. Also, the screw shaft mechanism was designed to move up and down in order to apply the load at varying rates. The speed rate was determined using the YASKAWA electrical system (AC Inverter) between 0.25 and 2.5 mm/min.

2.3 Test Procedure

Sand was poured into the test container using the raining fall technique. The unit weight of the sand (or relative density) can be achieved using this technique by adjusting the drop height and sand discharge rate (Turner and Kulhawy, 1987). Five trials were conducted in this regard to determine various values of the sand density using the raining technique. Sand was poured at various dropping heights to achieve a desired volume (i.e., 100, 200, 300, 400, and 500 mm). The results indicated that the weight of sand required to fill the required volume increased in direct proportion to the height of the drop, implying a direct relationship between the

sand density at a particular boundary and the drop's height. To determine the drop height in relation to the required sand density, a calibration curve was created. The height of the sand free fall was adjusted to maintain a constant sand discharge rate by adjusting the elevation of the hopper from the edge of the sand layer. In this study, loose and dense dry sand with relative densities of 30% and 80%, respectively, are considered. In this case, the density of sand was predetermined to correspond to a specific relative soil density. The test procedure and preparation steps used during the testing program are depicted in Figure 5.

(a)

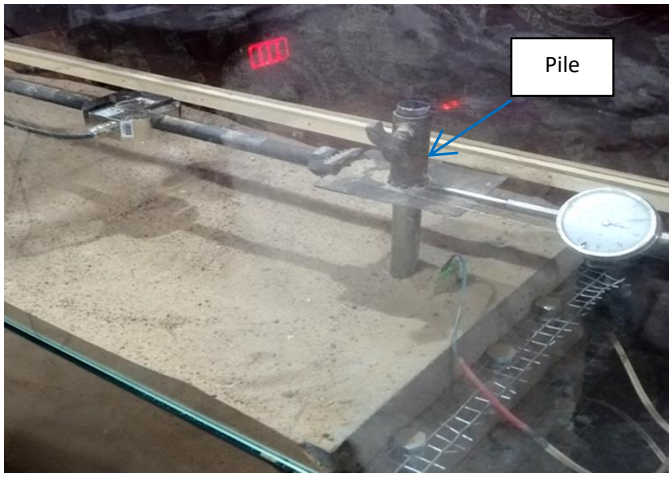

(b)

Figure 4 Lateral loading application system: (a) gear box and steel frame and (b) model of pile foundation subjected to lateral loads

The preparation steps include the following: (1) the BRC layers were cut and inserted into the pile's upper section via offset holes, and the pile was vertically positioned at its designated location. At the top of the test container, a frame of steel-section was fixed to locate the model of the pile at the mid-point, the pile was installed vertically through a cylindrical cavity with a diameter of 2 mm larger than the pile diameter, and then it was fixed with screws, (2) the wall facing was constructed by aligning rows of concrete panels at the required spacing between the BRC layers, (3) sand of a predetermined weight was added to the test container using the raining fall technique, taking into account the required depths of the BRC layers in the sand bed and (4) once the wall reaches its full height, the steel bar is removed from the pile and the loading mechanism is connected to the pile. During the test, a lateral load was applied, and the lateral displacement of the flexible pile was measured with a dial gauge with an accuracy of 0.001 mm. Additionally, a sensor system was used to determine the stress applied to the wall.

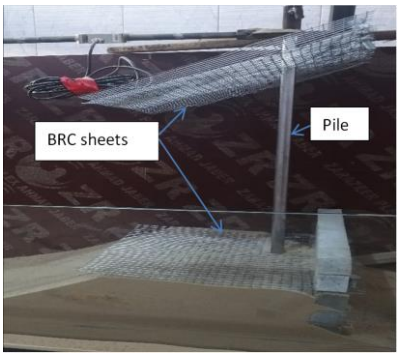

(a)

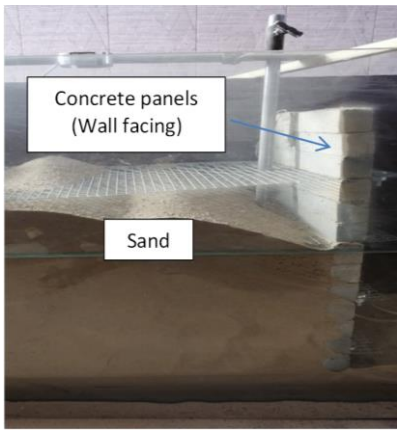

(b)

Figure 5 Test procedure: (a) pile alignment and (b) construction of the model

3. TEST RESULTS AND DISCUSSION

The scale effect was considered in this study for the small-scale models, take into consideration the formation of shear zones in the active zone directly beneath the footing. To avoid the particle size effect, Kusakabe (1995) recommended using a model with a ratio of pile diameter to mean particle size (D/D_{50}) of 50–100. As a result, the ratio of (D/D_{50}) was set at 60.3 in this study to minimize the scale effect. Twenty-two models were evaluated to determine the effects of several factors on the lateral capacity of the flexible pile and the applied pressure on the MSE retaining wall. For example, the slenderness ratio, the pile offset, the sand density, the type of connection, and the reinforcement length. However, the ultimate lateral resistance of piles was determined using the single tangent method from the load-deflection curve (Chawhan et al., 2012).

The present study considered two major groups: group (A) and group (B), referred to as the test group. Group (A) refers to the tests conducted on the flexible pile embedded in loose sand (Dr = 30%), whereas group (B) refers to the tests conducted on the flexible pile embedded in dense sand (Dr = 80%).

3.1 Effect of the Slenderness Ratio and Pile Offset on the Lateral Resistance of Pile and Applied Pressure on MSE Wall

The two groups were tested in two stages; the first stage included tests with various pile offsets (2D, 4D, and 6D) for each slenderness ratio (L/D). The second stage examined the behavior of the flexible pile for a given value of the pile offset at various values of the slenderness ratios (19.3, 21.7, and 24.1). The load-displacement curves for various pile offsets and slenderness ratios for groups (A) and (B) are shown in Figures 6 and 7. These tests were conducted with a reinforcement length of 315 mm (i.e., 0.7H), 90 mm vertical spacing between the reinforcement layers, and a mechanical connection between the reinforcement layers and the retaining wall facing.

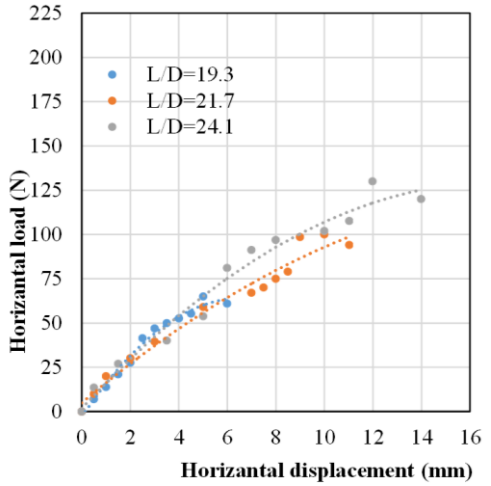

(a)

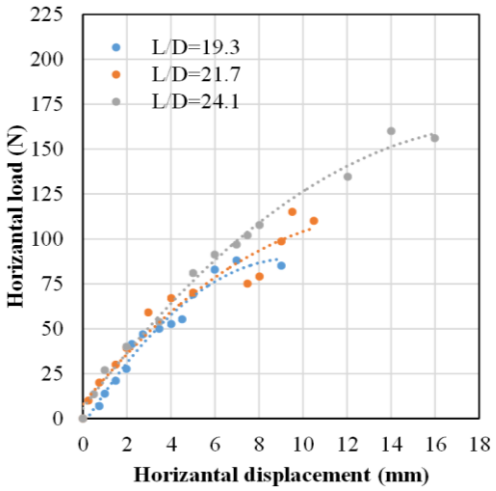

(b)

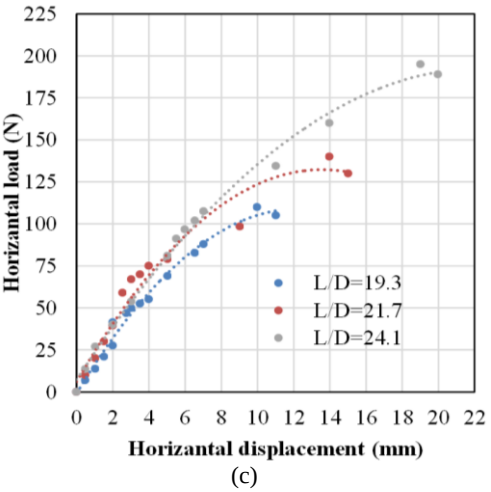

(c)

Figure 6 Lateral load-displacement curves of pile for group (A) with different values of pile offset: (a) 2D, (b) 4D, and (c) 6D

In the case of group (A), the ultimate capacity of lateral resistance of the flexible pile increased as the pile offset or L/D increased. When the L/D ratio is 19.3, the ultimate capacity of lateral resistance of the flexible pile increases with a pile offset of 6D to 66.7% and 26.8%, compared to the pile offsets of 2D and 4D, respectively. Additionally, for a 2D pile offset, the ultimate capacity of lateral resistance of the flexible pile increased from 100% to 57% in the case of L/D = 24.1 compared to the L/D of 19.3 and 21.7, respectively. For group (B), the ultimate capacity of lateral resistance of the flexible pile with an L/D of 24.1, increased by 40% and 20.6% for the pile offset of 6D, when compared to pile offsets of 2D and 4D, respectively. Furthermore, the ultimate capacity of lateral resistance of the flexible pile with L/D of 24.1 increased to 47% when compared to L/D = 21.7 for a 2D pile offset. While it was increased to 56% for a pile with an L/D of 21.7 compared to an L/D of 19.3.

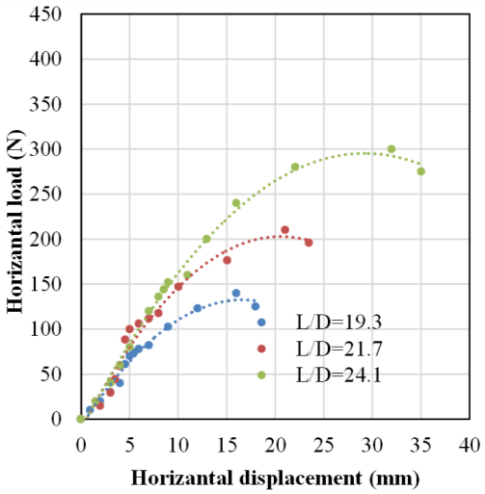

(a)

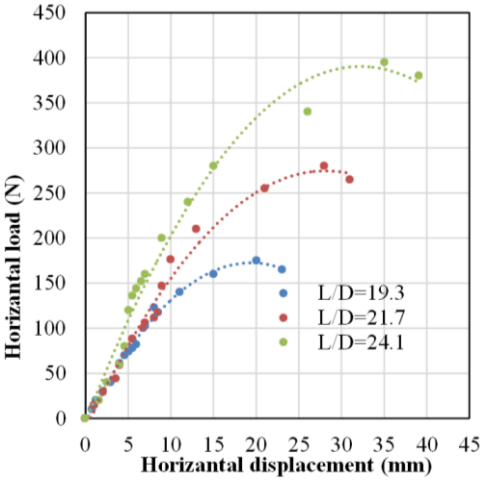

(b)

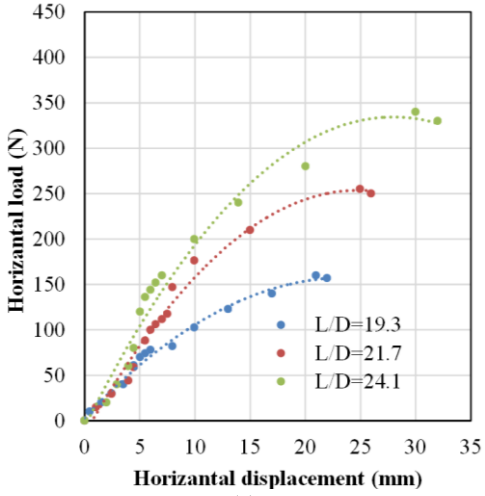

(c)

Figure 7 Lateral load-displacement curves of pile for group (B) with different values of pile offset: (a) 2D, (b) 4D, and (c) 6D

The stress-time curves for several testing groups with variable pile offsets (2D, 4D, and 6D) are depicted in Figures 8, 9, 10, and 11. The ultimate pressures of the stress-time curve were determined using pressure sensors located at a distance equal to 75% of the wall

height for group (A) and 25%, 50%, and 75% of the wall height for group (B).

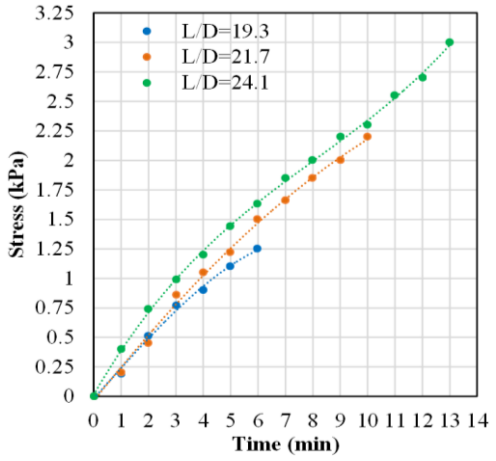

(a)

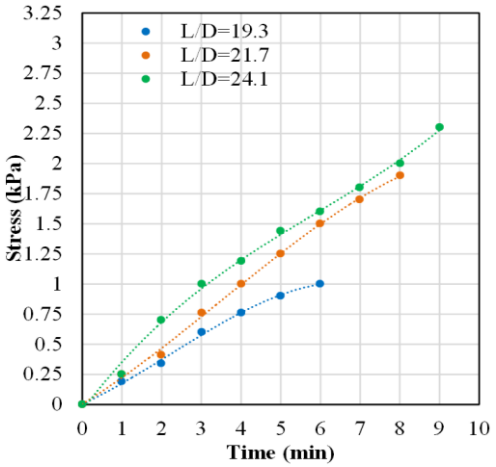

(c)

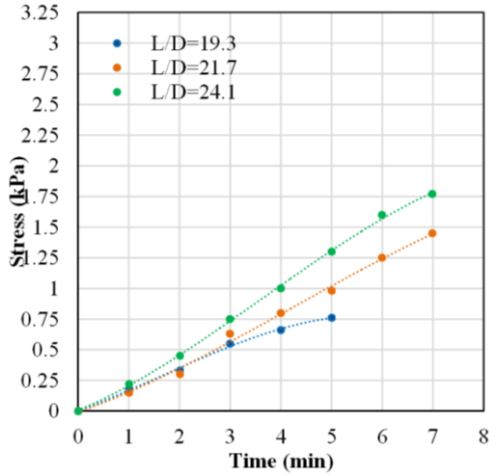

(c)

Figure 8 Stress-time curve of MSE retaining wall for group (A) with different values of pile offset: (a) 2D, (b) 4D, and (c) 6D

The results revealed that the pressure on the retaining wall decreases with the increasing offset of the piles. This behavior can be attributed to the increase in the distance between pile and wall facing, which can result in a significant reduction in the pressure applied to the retaining wall. In contrast, the applied pressure to the retaining wall increases as the ratio of L/D increases, owing to an increase in lateral earth pressure as a result of soil resistance to the lateral pile deflection and an increase in the transmitted pressure to the retaining wall. In group (B), for purposes of comparison, the pressure on the wall increased with increasing L/D when the pile offset was closer with regard to the wall facing, where the soil in this zone was highly compressed as a result of the soil resistance to the large deflection of the pile subjected to lateral loading.

The results of groups (A) and (B) for the behavior of flexible piles with varying slenderness ratios and pile offsets from the retaining wall facing are summarized in Tables 3 and 4, respectively.

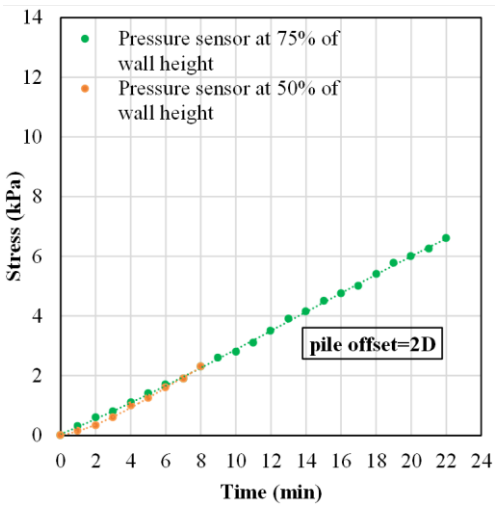

(a)

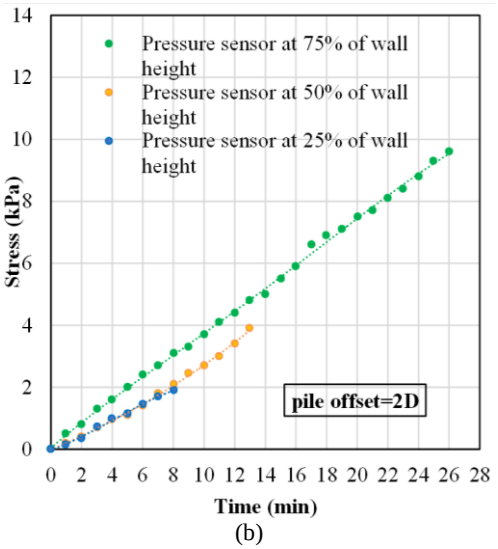

(b)

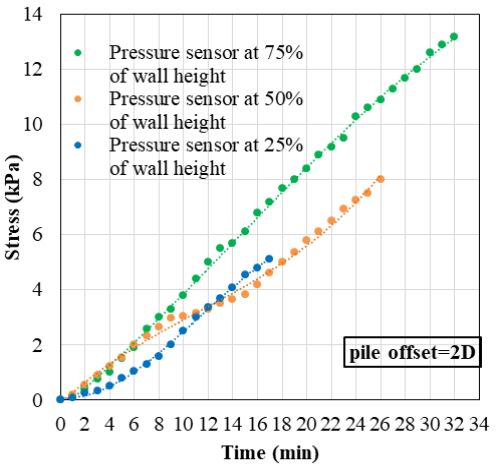

(c)

Figure 9 Stress-time curve of MSE retaining wall for group (B) with pile offset of 2D: (a) L/D = 19.3, (b) L/D = 21.7, and (c) L/D = 24.1

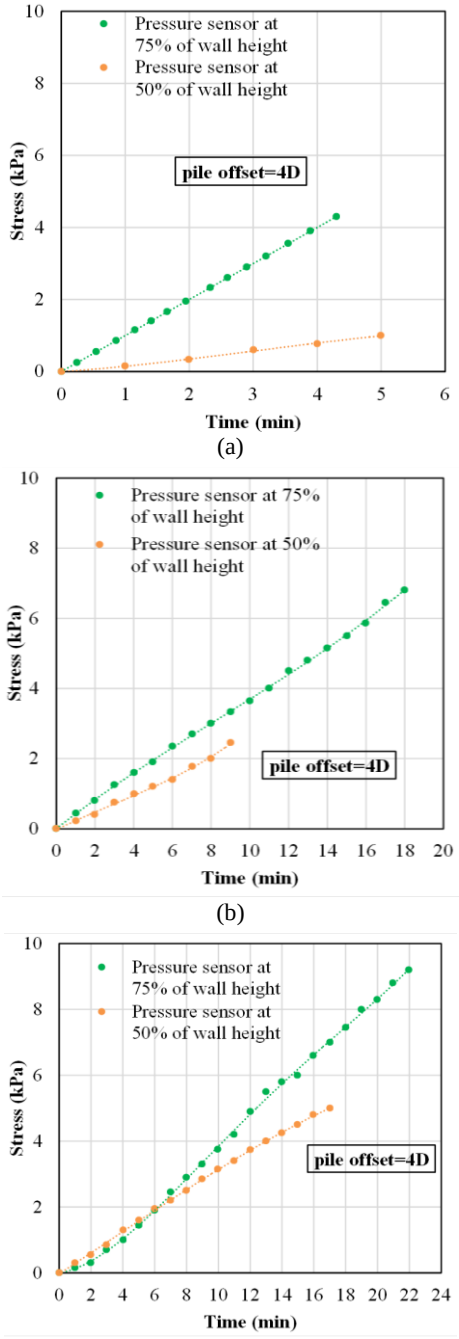

Figure 10 Stress-time curve of MSE retaining wall in group (B) at pile offset (4D) for: (a) L/D = 19.3, (b) L/D = 21.7, and (c) L/D = 24.1

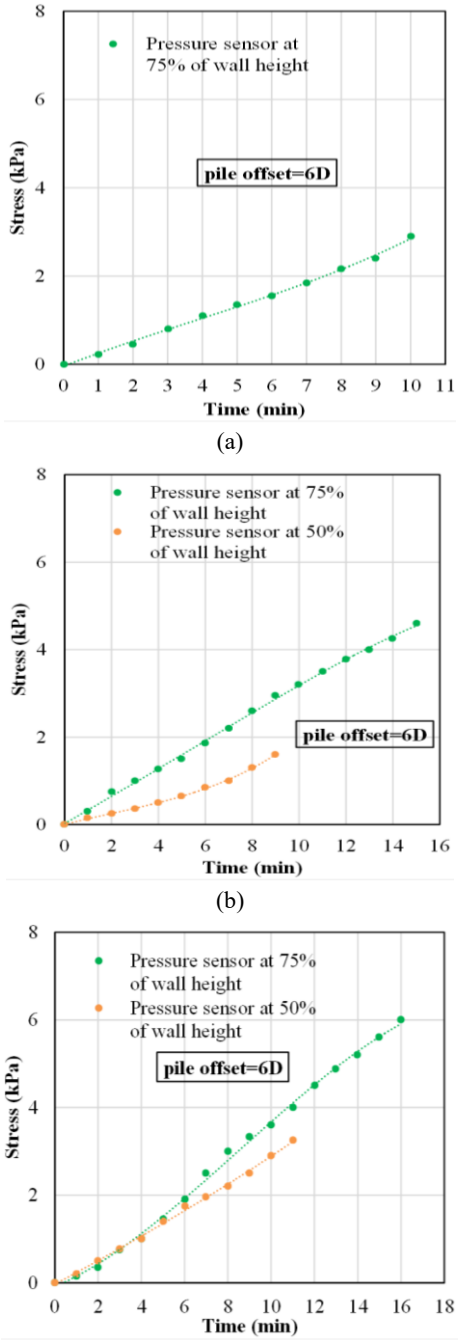

Figure 11 Stress-time curve of MSE retaining wall in group (B) at pile offset (6D) for: (a) L/D = 19.3, (b) L/D = 21.7, and (c) L/D = 24.1

Table 3 Summary of test results of group (A) to investigate the effect of slenderness ratio and pile offset

L/D	Pile offset (mm)	Ultimate lateral load (N)	Maximum pressure on the wall (kPa)		
			sensors at 75%H	sensors at 50%H	sensors at 25%H
19.3	41 (2d)	109	6.6	2.3	
19.3	82 (4d)	128	4.3	1	
19.3	123 (6d)	144	2.9		
21.7	41 (2d)	170	9.6	3.9	1.9
21.7	82 (4d)	210	6.8	2.45	
21.7	123 (6d)	250	4.6	1.6	
24.1	41 (2d)	250	13.2	8	5.1
24.1	82 (4d)	290	9.2	5	
24.1	123 (6d)	350	6	3.25	

Table 4 Summary of test results of group (B) shows the effect of slenderness ratio and pile offset

L/D	Pile offset (mm)	Ultimate lateral load (N)	Maximum pressure on the wall (kPa) (sensors at 75%H)
19.3	41 (2d)	51	1.25
19.3	82 (4d)	67	1
19.3	123 (6d)	85	0.76
21.7	41 (2d)	65	2.2
21.7	82 (4d)	80	1.9
21.7	123 (6d)	102	1.45
24.1	41 (2d)	102	3
24.1	82 (4d)	125	2.3
24.1	123 (6d)	135	1.77

3.2 Effect of Relative Density on Pile Lateral Capacity and Pressure on MSE Retaining Wall

The relative density of the sand bed in this section varied between loose and dense, corresponding to groups (A) and (B). At an L/D of 19.3, a pile offset of 2D, a reinforcement length of 315 mm with vertical spacing of 90 mm, and mechanical connection between BRC and retaining wall facing, the effect of relative density of sand on the lateral pile capacity was studied. The load-displacement curve of the pile under lateral loads and pressure on the retaining wall are shown in Figure 12 for various sand densities.

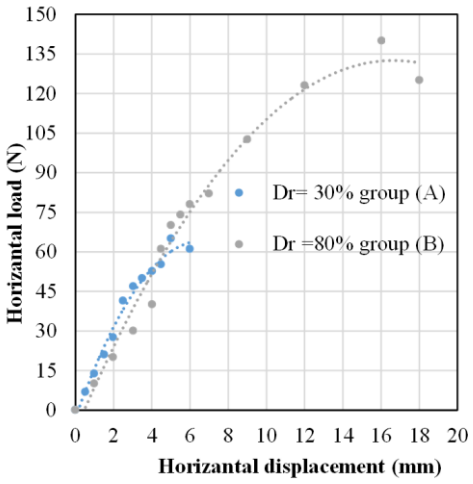

(a)

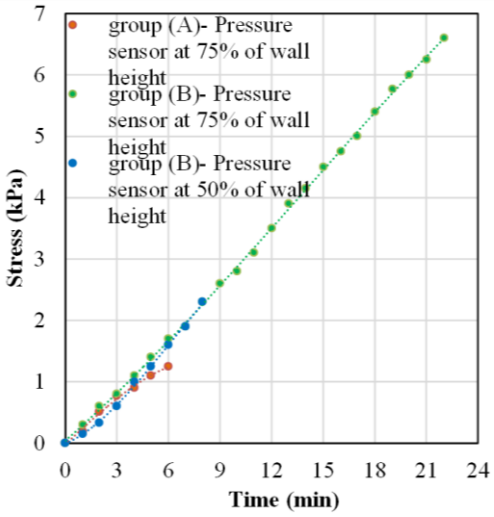

(b)

Figure 12 Effect of soil density on: (a) Lateral loads-displacement curve of pile and (b) stress-time curve

The results indicated that increasing the relative density of the sand increased the ultimate capacity of lateral resistance of the flexible pile. The ultimate lateral load on the pile in group (B) was increased to 113.7% greater than the ultimate lateral load on the pile in group (A). Increases in relative density also resulted in an increase in the pressure acting on the retaining wall. Thus, for the same L/D, the ultimate pressure developed on the wall of group (B) was greater than that developed on the wall of group (A). As a result, high pressure zones formed at 50% and 75% of the wall height in the case of group (B). Table 5 summarizes the test results for groups A and B with varying sand densities.

3.3 Effect of Connection Type on Pile Lateral Capacity and Pressure on MSE Retaining Wall

This section discusses two forms of connections (mechanical and frictional) between BRC layers and retaining wall facings. According to Figure 13, mechanical connections give greater resistance to lateral deflection of the flexible pile than frictional connections do with an L/D of 24.1, a pile offset of 2D, a reinforcement length of 315 mm (i.e., 0.7H), and 90 mm vertical spacing. As a result, an increase in the flexible pile's ultimate lateral load capacity was observed. For comparison, the ultimate capacity of lateral resistance of the flexible pile for group (B) with mechanical connections was 25% larger than the ultimate capacity of lateral resistance of the flexible pile with frictional connections. As indicated in Figures 14 and 15, the maximum pressure on the retaining wall in both test groups was greater in the case of mechanical connection than in the case of frictional connection. Because the mechanical connection provides greater resistance to pile lateral displacement, a greater force is required to generate additional wall deflection. Table 6 summarizes the test results for two distinct connection types.

Table 5 Summary the test results of ultimate capacity of pile and pressure on the wall for different densities of sand

Sand density	L/D	Ultimate lateral load (N)	Maximum pressure on the wall (kPa)	
			sensors at 75%H	sensors at 50%H
Group A	19.3	51	1.25	
Group B	19.3	109	6.6	2.3

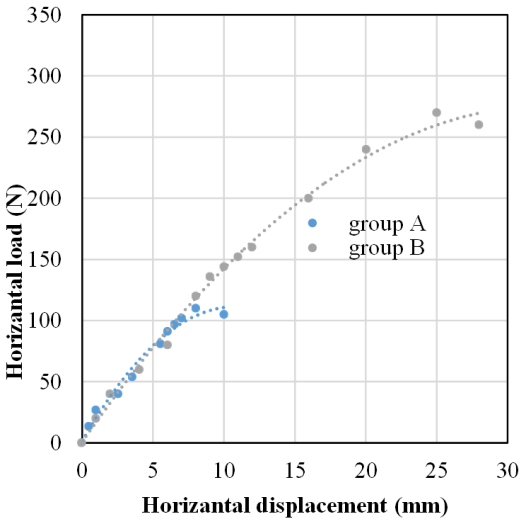

(a)

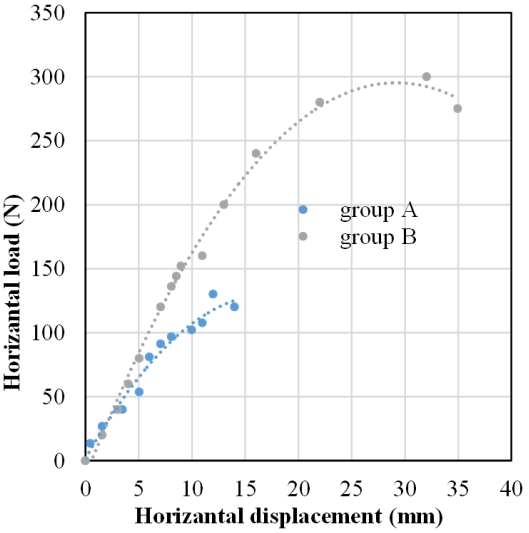

(b)

Figure 13 Lateral load-displacement curve of pile in sand with different test groups at L/D of 24.1 corresponding to: (a) frictional connection and (b) mechanical connection

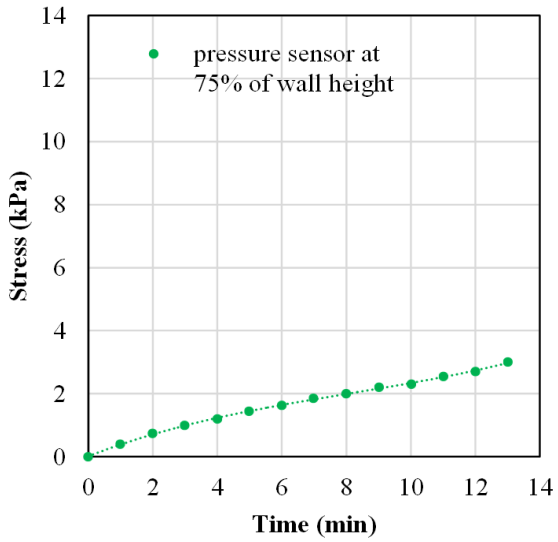

(a)

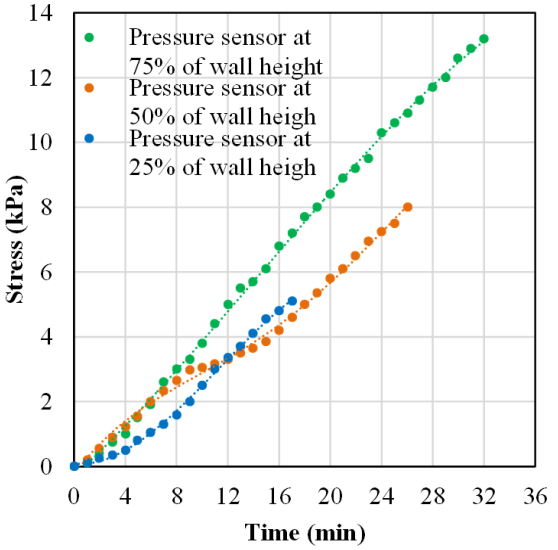

(b)

Figure 14 Stress-time curve of MSE retaining wall in sand with mechanical connection at L/D of 24.1 for: (a) group (A) and (b) group (B)

3.4 Effect of Length of Reinforcement on Pile Lateral Capacity and Pressure on MSE Retaining Wall

This section studies the influence of reinforcing length on the lateral capacity of flexible piles placed within the MSE retaining wall system. Two reinforcement lengths were investigated: a standard length of 315 mm (i.e., 0.7H) and a long length of 504 mm (i.e., 1.12H) at 90 mm layer spacing (i.e., twice the height of the single-wall panel (2Hp), with a 2D pile offset. Additionally, the experimental models incorporated the mechanical connection. The effect of reinforcing length on the pile's lateral capacity is depicted in Figure 16. Increased BRC length adds additional resistance to the pile against lateral deflection, resulting in an increase in the flexible pile's ultimate lateral load capacity. The ultimate lateral load capacity of group (A) was 37.3 percent greater with a reinforcement length of 504 mm than with a reinforcement length of 315 mm.

Figure 17 depicts the pressure applied to an MSE retaining wall with two different lengths of reinforcement.

It can be seen from Figure 17 that the maximum pressure occurs when a reinforcement length of 504 mm is used in comparison to a reinforcement length of 315 mm for both groups. In addition to reducing the wall-facing deflection, increasing the length of the reinforcement also increases the amount of earth pressure applied to the MSE retaining wall. The detailed results for both groups with varying reinforcing lengths are shown in Table 7.

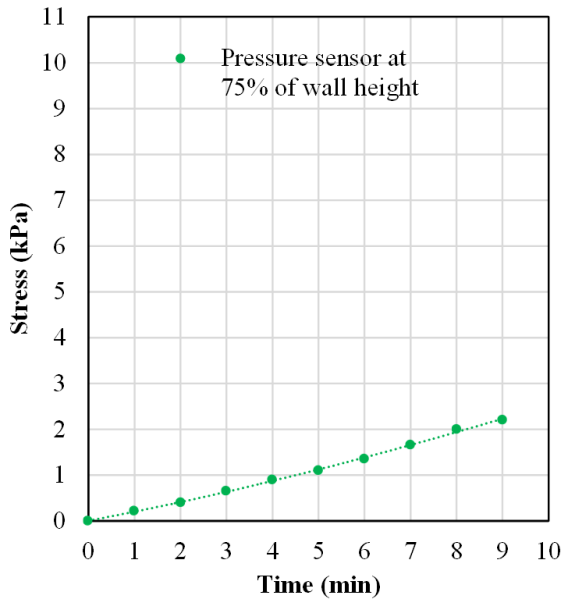

(a)

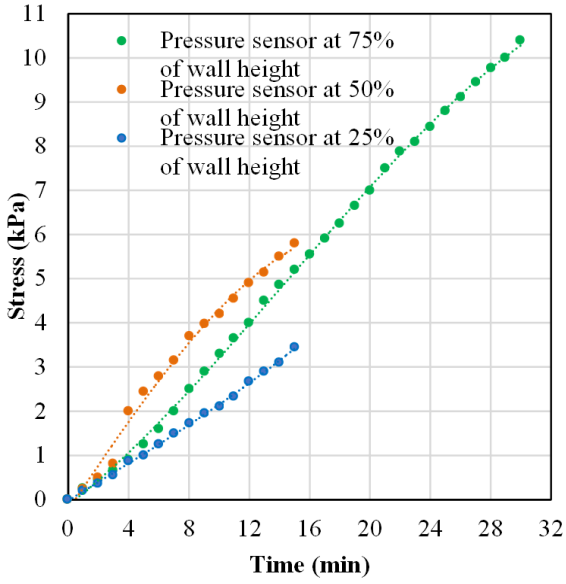

(b)

Figure 15 Stress-time curve of MSE retaining wall in sand with frictional connection at L/D of 24.1 for: (a) group (A) and (b) group (B)

Table 6 Summary of test results pertaining to connection type between BRC and wall facing

Group	L/D	Connection Type	Ultimate lateral load (N)	Maximum pressure on the wall (kPa) when sensors located at:		
				75% H	50%H	25% H
A	24.1	mechanical	102	3		
B	24.1	mechanical	250	13.2	8	5.1
A	24.1	frictional	82	2.2		
B	24.1	frictional	200	10.4	5.8	3.45

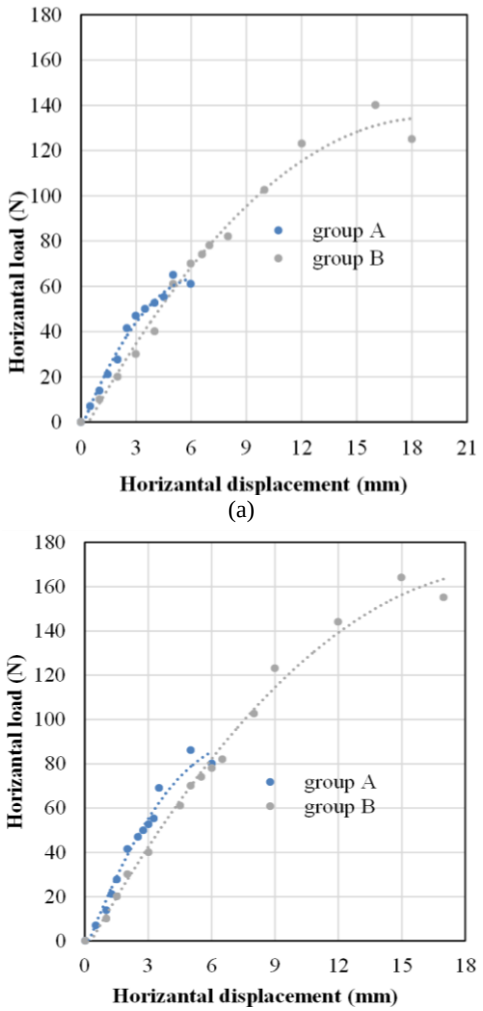

Figure 16 Lateral loads-displacement curve of pile in sand with different test groups at L/D of 19.3 for: (a) reinforcement length (315 mm) and (b) reinforcement length (504 mm)

4. CONCLUSIONS

Previous investigations have mostly focused on the behavior of rigid piles embedded within MSE wall systems. This study revealed the situation in which flexible piles are used in conjunction with an MSE retaining wall system. This paper looked into a number of parameters, including pile offset measured from the retaining wall facing, slenderness ratios (i.e., L/D), relative density of the sand bed, length of BRC reinforcement, and the type of connection used to connect the retaining wall facing and the BRC units. The following conclusions were reached based on the findings of the experimental tests:

1) An increase in sand density from loose to dense resulted in a significant increase in the lateral resistance of the flexible pile within the MSE retaining wall system. An increase in sand density also resulted in an increase in the pressure applied on the retaining wall.
2) A higher value of the slenderness ratio of the flexible pile resulted in greater lateral resistance of the pile for a specific relative density of sand.
3) An increase in the pile offset results in an increase in the lateral resistance of the flexible pile as well. When the offset reaches six times the pile diameter, the lateral resistance of the flexible pile increases to its maximum value. Increases in the pile offset, on the other hand, result in a reduction in the pressure on the MSE retaining wall.
4) When the length of the BRC reinforcement was increased, it was found that the ultimate lateral resistance of the flexible pile increased by a significant amount. Optimal reinforcement ratio was determined to be 1.12 times the height of the retaining wall.
5) When comparing the frictional connection used to connect the retaining wall facing and BRC reinforcement units to the mechanical connection, it is found that the frictional connection significantly reduces the ultimate lateral resistance of the flexible pile as well as the pressure on the MSE retaining wall.

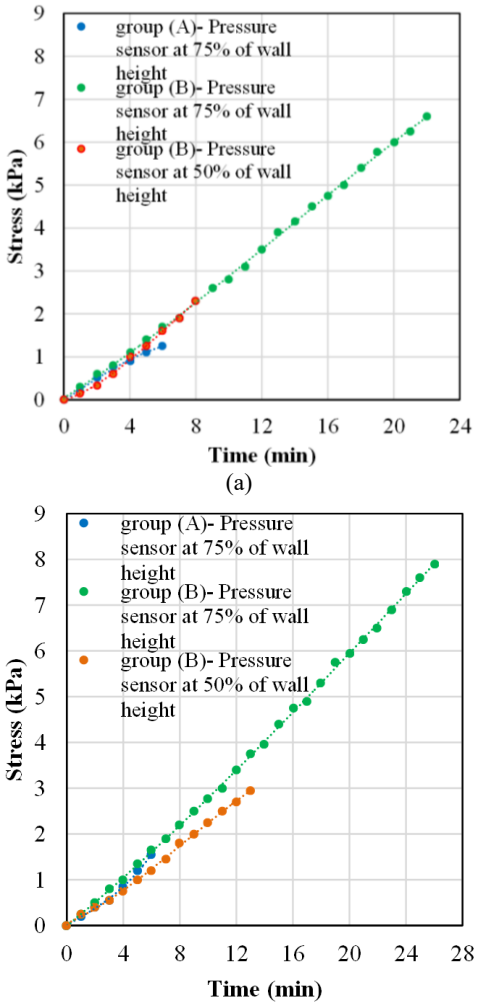

Figure 17 Stress-time curve at L/D of 19.3 for: (a) reinforcement length (315 mm) and (b) reinforcement length (504 mm)

Table 7 Summary of test results related to various reinforcement lengths within MSE retaining wall

Group	L/D	Reinforcement length (mm)	Ultimate lateral load (N)	Maximum pressure on the wall (kPa) at:	
				75%H	50%H
A	19.3	315	51	1.25	
B	19.3	315	109	6.6	2.3
A	19.3	504	70	1.55	
B	19.3	504	131	7.9	2.95

5. LIST OF NOTATIONS

D	diameter of pile
D_{10}	particle size at 10% finer by weight
D_{30}	particle size at 30% finer by weight
D_{50}	particle size at 50% finer by weight
D_{60}	particle size at 60% finer by weight
Dr	relative density
e	load eccentricity
L	embedded pile length
H	wall height
Hp	height of concrete panels of wall facing
MSE	mechanically stabilized earth
USCS	unified soil classification system

6. REFERENCES

ASTM D422-2001 "Standard Test Method for Particle Size-Analysis of Soils." American Society of Testing and Material.

ASTM D4253-00 (2006). "Standard Test Method for Maximum Index Density and Unit Weight of Soils Using a Vibratory Table." West Conshohocken, Pennsylvania, USA.

ASTM D4254-00 (2006). "Standard Test Method for Minimum Index Density and Unit Weight of Soils and Calculation of Relative Density." West Conshohocken, Pennsylvania, USA.

ASTM D3966-07 "Standard Test Method for Piles under Lateral Loads". Annual Book of ASTM Standards.

Berg, R. and Vulova, C. (2007). "Effects of pile driving through a full-height precast concrete panel faced, geogrid-reinforced, mechanically stabilized earth (MSE) wall", *Case Studies in Earth Retaining Structures*, 1-10.

Berg, R.R., Christopher, B.R., and Samtani, N.C. (2009). "Design of mechanically stabilized earth walls and reinforced soil slopes." FHWA, Washington, D.C., Report No. FHWANHI-10-024.

Chawhan, B.S., Quadri, S.S., and Rakaraddi, P.G. (2012). "Behavior of Lateral Resistance of Flexible Piles in Layered Soils." *IOSR Journal of Mechanical and Civil Engineering*, Volume 2, Issue 5: 07-11.

Elias, V., Christopher, B. R., and Berg, R. R. (2001). "Mechanically stabilized earth walls and reinforced soil slopes design and construction guidelines".

FHWA (2007). "Mechanically stabilized earth wall abutments for bridge support".

Han, J. (2014). "Lateral resistance of piles near 15-foot vertical MSE abutment walls reinforced with ribbed steel strips." M.Sc. thesis, Department of Civil and Environmental Engineering, Brigham Young University.

Huang, J., Parsons, R. L., Han, J., and Pierson, M. (2011). "Numerical analysis of a laterally loaded shaft constructed within an MSE wall." *Geotextiles and Geomembranes*, 29(3), 233-241.

Jawad, S., Han, J., Al-Naddaf, M., and Abdulrasool, G. (2020). "Responses of laterally loaded single piles within mechanically stabilized earth walls." *Journal of Geotechnical and Geoenvironmental Engineering*, 146(12)., 04020128.

Khodair, Y. A. and Hassiotis, S. (2005). "Analysis of soil–pile interaction in integral abutment". *Computers and Geotechnics*, 32(3), 201-209.

Kusakabe, O. (1995). Chapter 6: foundations. Geotechnical centrifuge technology, 118-167.

Mohammed, W. K. (2016). "Factors influencing performance of a laterally loaded pile with an MSE wall system." M.Sc. thesis, Dept. of Civil, Environmental, and Architectural Engineering, University of Kansas, USA.

Nelson, K.R. (2013). "Lateral resistance of piles near vertical MSE abutment walls at Provo Center Street." M.Sc. Thesis, Department of Civil and Environmental Engineering, Brigham Young University, Provo, UT.

Pierson, M., Parsons, R.L., Han, J., Brown, D.A., and Thompson, W.R. (2009). "Capacity of laterally loaded shafts constructed behind the face of a mechanically stabilized earth block wall." Kansas Department of Transportation, K-TRAN: KU-07-6.

Price, J. S. (2012). "Lateral resistance of piles near vertical MSE abutment walls." Master of Science, Brigham Young University, Provo, UT.

Rollins, K. M., Price, J. S., and Bischoff, J. (2011). "Lateral resistance of piles near vertical MSE abutment walls." *Geo-Frontiers: Advances in Geotechnical Engineering*, 3526-3535.

Rollins, K., Price, J., and Bischoff, J. (2012). "Reduced lateral resistance of abutment piles near MSE walls based on full-scale tests." *International Journal of Geotechnical Engineering*, 6(2), 245-250.

Rollins, K.M. and Nelson, K., (2015). "Influence of pile offset behind an MSE wall on lateral pile resistance." *Proceedings of the XVI European Conf. on Soil Mech. and Geotech. Engineering: Geotechnical Engineering for Infrastructure and Development*, ICE publishing, 1163-1168.

Sharma, B. (2011). "A model study of micro piles subjected to lateral loading and oblique pull." *Indian Geotechnical Journal*, 41(4), 196-205.

Turner, J. P. and Kulhawy, F. H. (1987). "Experimental analysis of drilled shaft foundations subjected to repeated axial loads under drained conditions." (No. EPRI-EL-5325). Cornell Univ., Ithaca, NY (USA). Geotechnial Engineering Group; Electric Power Research Inst., Palo Alto, CA (USA).

Wilson, P., Lee, A. and Law, H. (2016). "Analysis of laterally-loaded piles in MSE embankments." *In Geotechnical and Structural Engineering Congress*, 138-150.